**ISSN: 0067-2904**

# Study of Plasma Diffusion in DC Glow Discharge Using Optical Emission Spectroscopy

**Murad M. Kadhim*, Qusay A. Abbas**
*Physics Dep., College of Science, University of Baghdad, Baghdad, Iraq*

Received: 30/9/2024 Accepted: 4/3/2025 Published: 30/3/2026

**Abstract**

This study focused on plasma diffusion to understand how gas pressure affects diffusion dynamics. Experimental measurements were carried out to assess the electron temperature, electron number density, drift velocity, particle flux, growth rate, diffusion coefficient, and constant time decay as a function of gas pressure. The results showed that while the electron number density ($n_e$) grows with increased gas pressure, the electron temperature ($T_e$) of the plasma falls. The results indicated that gas pressure significantly influences plasma behavior, with a notable decrease in diffusion coefficients and constant time decay as gas pressure rises from 0.04 to 0.4 mbar. The stability and diffusivity of the plasma are affected by bumping effects, which are enhanced by increased gas pressure. This study advances our knowledge of plasma behavior in DC glow-discharge systems by emphasising the relationship between gas pressure and plasma dispersion.

**Keywords**: Glow discharge, EXB drift, Diffusion coefficient, Constant time decay, Growth rate, Particle flux

# دراسة انتشار البلازما في تفريغ التوهج للتيار المستمر باستخدام مطياف الانبعاث البصري

**مراد محمد كاظم*, قصي عدنان عباس**
قسم الفيزياء, كلية العلوم, جامعة بغداد، بغداد، العراق

**الخلاصة**

ركزت هذه الدراسة على انتشار البلازما لفهم كيفية تأثير هذه المعلمات (مثل ضغط الغاز) على ديناميكيات الانتشار. تم إجراء قياسات تجريبية لتقييم درجة حرارة الإلكترون، الكثافة العددية للألكترونات، سرعة الانجراف، تدفق الجسيمات، معدل النمو، معامل الانتشار، والتحلل الزمني الثابت كدوال لضغط الغاز. أظهرت النتائج أنه بينما تنمو الكثافة العددية للإلكترونات ($n_e$) مع زيادة ضغط الغاز، تنخفض درجة حرارة الإلكترون ($T_e$) للبلازما مع زيادة ضغط الغاز. تشير النتائج إلى أن ضغط الغاز يؤثر بشكل كبير على سلوك البلازما، مع انخفاض ملحوظ في معاملات الانتشار والانحلال الزمني الثابت مع ارتفاع ضغط الغاز من 0.04 إلى 0.4 ملي بار. يتأثر استقرار وانتشار البلازما بتأثيرات الارتطام، والتي تتعزز بزيادة ضغط الغاز. من خلال تسليط الضوء على العلاقة بين ضغط الغاز وتشتت البلازما، تعمل هذه الدراسة على تعزيز معرفتنا بسلوك البلازما في أنظمة التفريغ المتوهج للتيار المستمر.

*Email: murad.kadhim1204@sc.uobaghdad.edu.iq

## 1 Introduction

DC (DC) glow discharge is usually considered a reliable source of plasma formation, especially in applications that ask for accurate control over plasma properties, such as electron temperature, electron density and symmetry [1]. The main purpose of the ionization process is to induce an electric field in the chamber that accelerates free electrons and affects gas atoms or molecules [2, 3]. For example, planar electrodes can effectively spread plasma in large surface areas. Plasma diffusion refers to the process where charged particles (electrons and ions) in a plasma move from a region of high concentration (or density) to a region of lower concentration. This plays a crucial role in maintaining uniformity, while also influencing the characteristics and density of all other diffusion processes. For glow discharge systems, the diffusion process is highly significant [4]. The planar electrodes' extremely high efficiency and ease of use make them highly appealing for applications associated with a lot of plasma processing, such as semiconductor fabrication and thin-film deposition. The complex growth behavior results from the electric field generated by the externally applied DC voltage, combined with the physical constraints imposed on the planar electrodes due to particle interactions in the plasma [5, 6]. The characteristics of plasma discharge in a DC glow discharge system are influenced by multiple factors, including gas quantity and voltage amplitude. It is thus important to consider some mechanical operation parameters, such as pressure, magnetic field strength, plasma density, electric field, temperature, and electrode configuration, that contribute to a better understanding of the diffusion processes. Increasing the plasma symmetry will also improve the efficiency of the DC glow discharge system [7, 8].

The aim of this paper is to investigate and analyze plasma diffusion in a DC glow discharge using optical emission spectroscopy, focusing on the spectral characteristics of plasma behavior in such systems, including electron temperature, electron number density, and Debye length.

## 2. Theoretical consideration

### 2.1 Plasma Parameters

Optical emission spectroscopy (OES) is the most sensitive method for plasma detection. It stores plasma information, such as electron density and temperature [9]. The Boltzmann plot technique is the most widely used method for determining the electron temperature ($T_e$). Local thermodynamic equilibrium (LTE) is assumed when the Boltzmann distribution is satisfied. This approach is well-liked and simple for spectroscopic measurements [10, 11]. Boltzmann plot is constructed from the following equation:

$$\ln\left(I_{ji}\,\lambda_{ji}/A_{ji}\,g_j\,hc\right) = -E_j/k_B T_e + \ln(N/U) \quad (1)$$

The transition intensity, wavelength, and transition probability from level $j$ to level $i$ are represented by the variables $I_{ji}$, $\lambda_{ji}$, and $A_{ji}$, respectively. Where $g_j$ is the statistical weight, $h$ is Planck's constant, $c$ is the speed of light, $E_j$ is the energy of the upper level j, $k_B$ is Boltzmann's constant, N is the numerical density of the emitting species, and U is the partition function.

The electron number density ($n_e$) is calculated by utilizing the Stark broadening effect, which necessitates a spectral line unaffected by self-absorption[12, 13]:

$$n_e = \left[\frac{\Delta\lambda}{2\omega_s}\right] N_r \quad (2)$$

The term $\Delta\lambda$ refers to the Full Width at Half Maximum (FWHM) of the spectral line while $\omega_s$ denotes the theoretical Stark broadening parameter corresponding to the

reference electron density $N_r = 10^{16}$ ($cm^{-3}$) [14]. The potential resulting from the thermal oscillation of highly mobile electrons is shielded to a distance called the Debye length ($\lambda_D$). The Debye length in the plasma can be obtained by equality the kinetic energy of the thermal electrons with resulting electrostatic potential as follows [15]:

$$\lambda_D = \sqrt{\frac{\varepsilon_0 \, k_B \, T_e}{e^2 \, n_e}} \tag{3}$$

where $\varepsilon_0$ is the permittivity of free space, $k_B$ is Boltzmann's constant, and $T_e$ is the temperature of the electrons, with other symbols having previous definitions. Such quantification provides a clear overview of plasma electron heating mechanisms and highlights the role of specific physical interactions, such as collisional energy transfer, in the presence of external fields.

**2.2 Plasma Diffusion**

The combined influence of electric and magnetic fields on particle velocities in a plasma gives the $E \times B$ drift velocity. It does not depend on the mass or charge of the particle undergoing drift. The $E \times B$ drift velocity is given by the equation [16]:

$$V_{E\times B} = \frac{E\times B}{B^2} = \frac{E}{B} = \frac{k_B T_e}{d\, eB} \tag{4}$$

Where $E$ represents the electric field, measured in volts per meter ($V/m$), it is the force per unit charge exerted on charged particles due to the electric field; $B$ represents the magnetic field, measured in Tesla ($T$); $d$ is the distance at the central region between the electrodes; and $B^2$ is the magnitude of the magnetic field squared. Collisions between charged particles in a plasma are crucial for diffusion processes. These interactions facilitate the transfer of momentum and energy, causing particles to shift and redistribute throughout the plasma. Bohm diffusion refers to the diffusion of plasma across a magnetic field ($B$), characterized by a diffusion coefficient given by [16]:

$$D_{Bohm} = \frac{1}{16} \frac{k_B T_e}{eB} \tag{5}$$

Where $k_B T_e$ is the thermal energy of electrons which drives diffusion, and $eB$ is the strength of the magnetic field, which opposes diffusion and confines the particles, and the factor 1/16 is empirical, derived from experiments and simulations of plasma diffusion.

In plasma studies, continuous matters often refer to specific time that occurs for a particular feature, such as the intensity or electron number density of an emission line, to decay a certain fraction of its original value. This decay is usually controlled by procedures such as recreation or relaxation; It is important to understand the extent of this time to analyze the behavior of plasma over time. The time constant for diffusion ($\tau$) is given by:

$$\tau = \frac{d^2}{(2.4)^2 \, D} \tag{6}$$

Where $D$ is the diffusion coefficient, and d is the distance from the cathode to the anode. It is observed from this equation that, the constant time decay $\tau$ is inversely proportional to $D$. This means that, the constant time decay of plasma has high values in the region of low diffusion coefficient and low in the high diffusion coefficient region [17, 18].

In the context of plasma diffusion and instabilities, the growth rate $\gamma$ can often be expressed as:

$$\gamma = \frac{D}{d^2} \tag{7}$$

The particle flux ($\Gamma$) per unit area per unit time $(m^2 \cdot s)^{-1}$ is determined by multiplying the particle density ($n$) by the mean velocity of the particles ($< v >$), according to the equation [19]:

$$\Gamma = n < v >= n \sqrt{\frac{8k_B T_e}{\pi m_e}} \quad (8)$$

Where: $m_e$ is the electron mass.

## 3. Experimental Part

The experimental setup of a system of planar electrodes in a vacuum chamber is illustrated in Fig. (1). The chamber, constructed from cylindrical Pyrex glass (37 cm in length and 30 cm in diameter), was evacuated to a base pressure of about $2\times10^{-2}$ mbar using a two-stage rotary pump, with the pressure monitored by a digital Pirani gauge. The Argon gas was introduced via one of two small pipes. The planar electrodes, made from aluminum (6 cm in diameter and 3 cm in length), were insulated with Teflon and positioned 10 cm apart. A 4kV DC voltage was applied to generate a standard glow discharge between the electrodes. Magnetic fields with strengths ranging from 1-3.4mT were generated using circular and ring-shaped magnets arranged axially (parallel to the plasma column). The distribution of these fields was measured using a Tesla meter. The spatially integrated plasma light emission was analyzed with an optical emission spectrometer (Thorlabs type- manufactured in Germany) to extract the parameters of the plasma radiation in the 320-740 nm wavelength range. The distance between the plasma and the spectrometer was 15 cm, with the spectrometer positioned at a 45-degree angle relative to the plasma column.

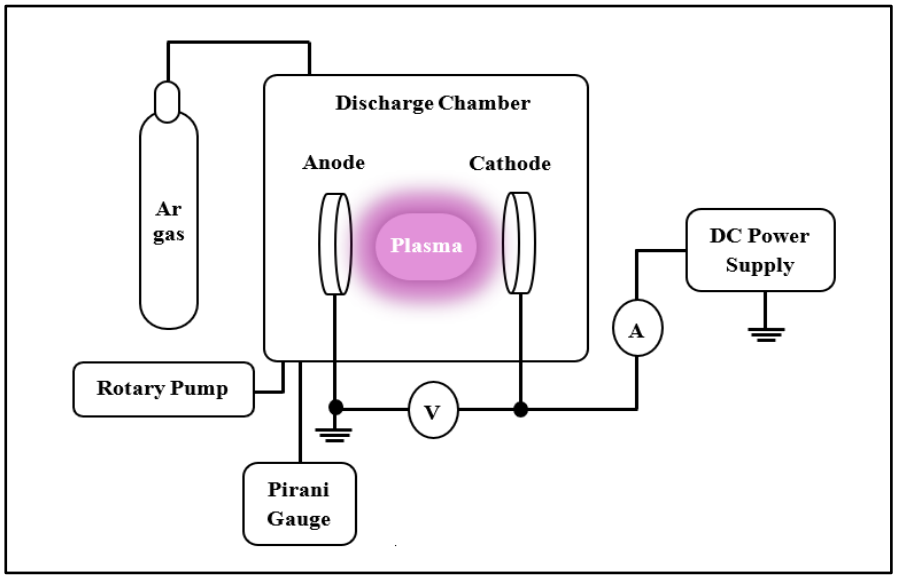


**Figure 1:** Diagram of the DC planar electrodes setup.

## 4. Results and Discussion

### 4.1 Emission Plasma Intensity

To analyze the emission spectrum of argon (Ar) plasma, spatially integrated light emission in the 320-740 nm wavelength range was examined with an optical emission spectrometer. This study provides valuable insights into the properties and behavior of plasma. Figure (2) shows the argon plasma emission spectrum at different gas pressures (0.04, 0.06, 0.08, 0.2, and 0.4 mbar) in a planar magnetron sputtering system. The figure reveals several peaks corresponding to the neutral ArI atom, observed at wavelengths of 357.69150, 419.15760, 486.13637, 549.58730, 603.21270, 617.30960, 656.51368, 675.28340, 696.53400, 706.87350, and 738.39800 nm. Additionally, ionic emission lines of AII were detected at wavelengths of 391.15760 and 427.75280 nm. The intensity of each peak increased as the gas pressure increased from 0.04 to 0.4 mbar. The reason for

this is a rise in the electron number density, which speeds up the rate at which electrons collide with the gas atoms, providing sufficient excitation. This result agrees with that reported by Bellan [20].

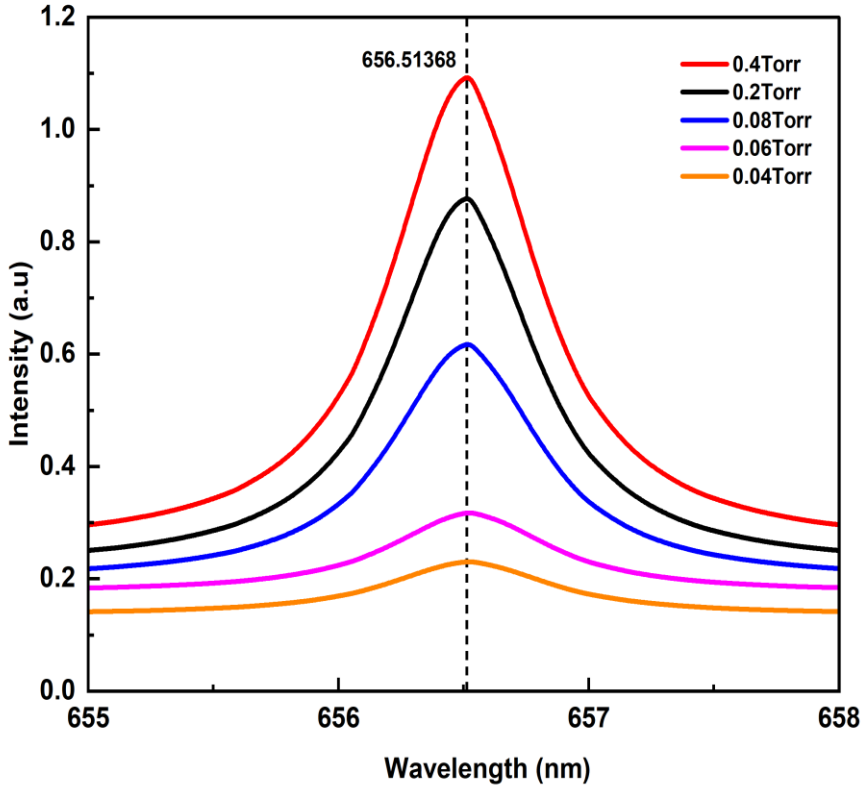


**Figure 2:** The optical emission spectra of argon plasma at various gas pressures.

### 4.2 Plasma Parameters

The slope of the best-fitting line of the Boltzmann plot, which is derived by plotting $\ln(\lambda_{ji} I_{ji}/hc\, g_j A_{ji})$ versus surface energy ($E_j$), according to Equation (1), can be used to calculate $T_e$. This approach requires data from the NIST database and peaks from the same atomic species, which are presented in Table (1). Figure (3) illustrates the Boltzmann plots with selected atomic argon lines (ArI) of a planar magnetron sputtering system at various gas pressures. The electron number density ($n_e$) was computed by Equation (2), with high accuracy using the spectral lines emitted by the atoms and ions in the plasma, as shown in Fig. (4), also known as the Stark broadening effect [21].

**Table 1:** ArI standard line characteristics used to determine $T_e$ [22].

| $\lambda$(nm) | $A_{ji} \times g_i$ | $E_i$(eV) | $E_j$(eV) |
|---|---|---|---|
| 549.58730 | $152\times10^5$ | 13.07571571 | 15.3310400 |
| 603.21270 | $221\times10^5$ | 13.07571571 | 15.13054437 |
| 617.30960 | $34\times10^5$ | 13.15314387 | 15.1610486 |
| 656.42224 | $7.7\times10^5$ | 13.07571571 | 14.97152236 |
| 706.87350 | $60\times10^5$ | 13.09487256 | 14.84836899 |

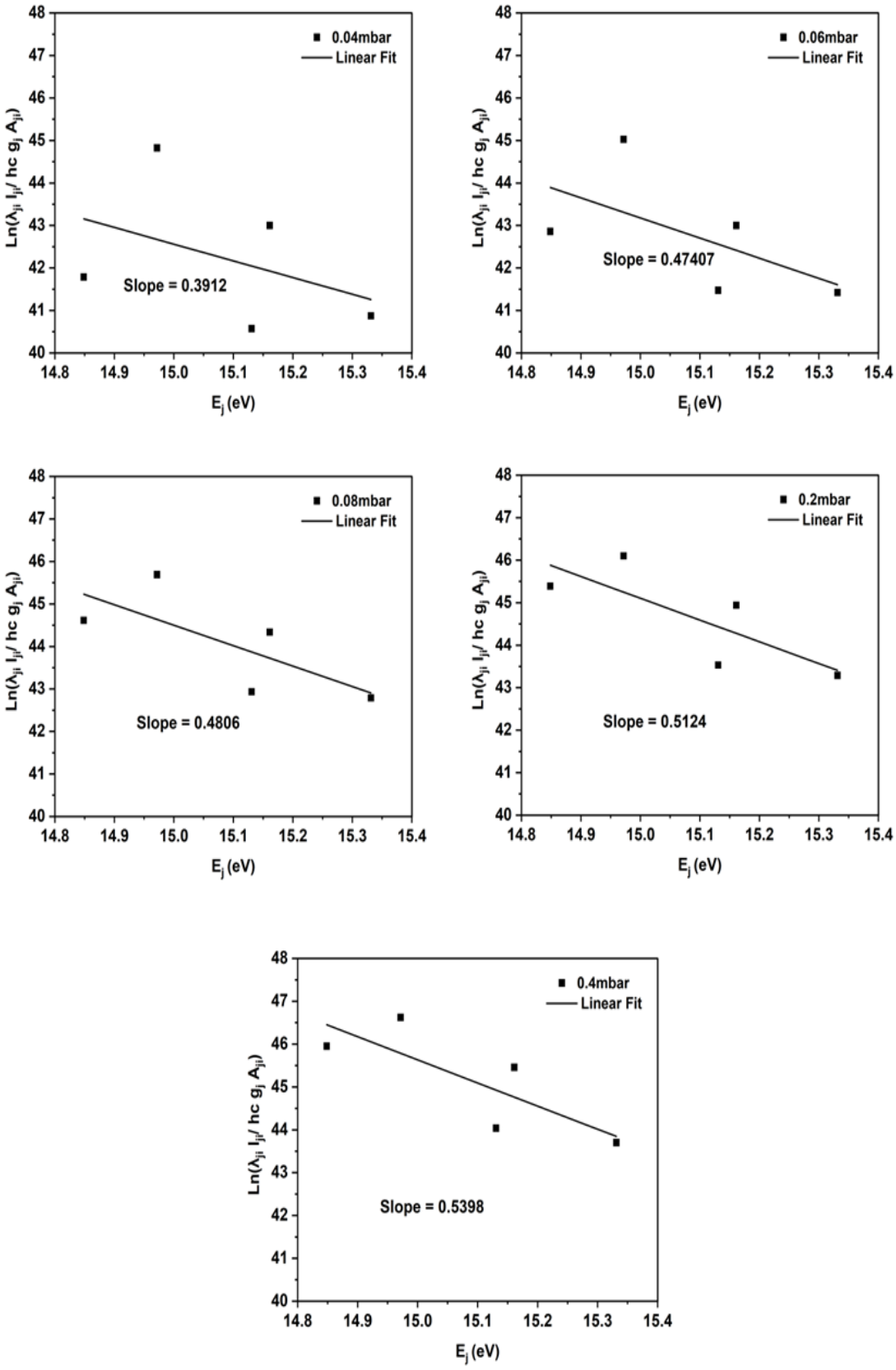


**Figure 3:** Boltzmann plot of ArI peaks for a magnetron sputtering system at various gas pressures.

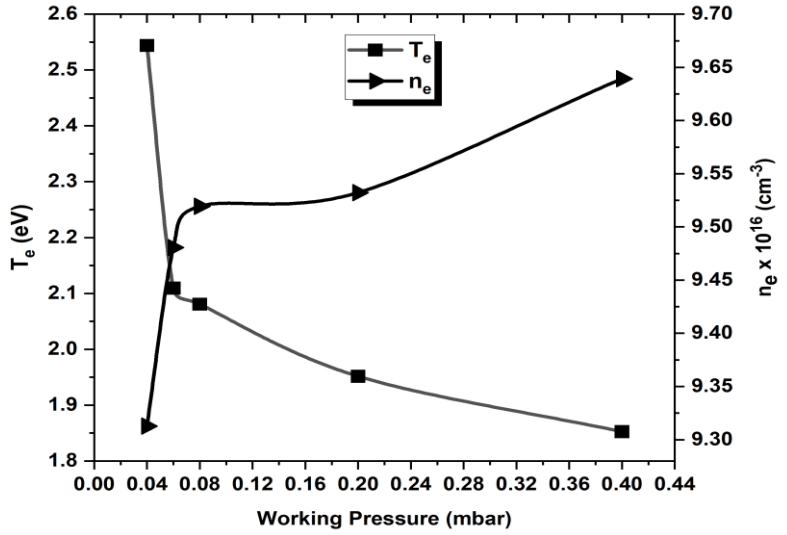


**Figure 4:** Stark broadening for 656.51368 nm at different gas pressures.

In a planar magnetron sputtering system, Figure (5) shows how the electron temperature ($T_e$) and electron density ($n_e$) change as the gas pressure changes. According to the findings, as the gas pressure rose from 0.04 to 0.4mbar, the electron temperature decreased, but the electron number density increased. At low gas pressures, electrons have long electron mean free paths, described by the equation $\lambda = v/n\sigma$ (where $\lambda$ is the mean free path, $v$ is the average electron velocity, $n$ is the gas atom number density, and $\sigma$ is the collision cross-section), which leads to fewer collisions and higher electron temperatures. As pressure increases, more collisions occur, causing energy loss and lowering electron temperatures [21]. Concurrently, these inelastic collisions increase ionization, thus increasing the electron number density. Therefore, high gas pressure increases electron number density from ionization while electron temperature decreases due to the higher collision rate [23].

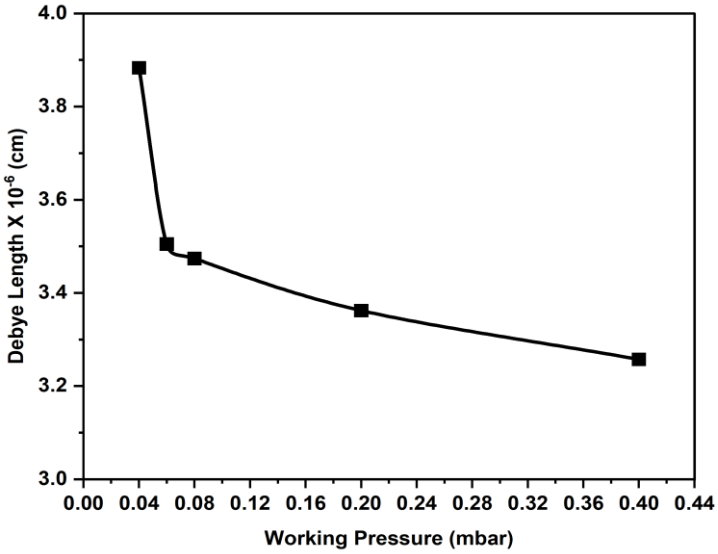


**Figure 5:** The variation of $T_e$ and $n_e$ with working pressure in planar magnetron sputtering system.

The Debye length ($\lambda_D$) was calculated and displayed in Figure (6) using Equation (3) and Figure (5). The findings demonstrated that the Debye length decreased when gas pressure increased from 0.04 to 0.4 mbar. These characteristics indicate that the decrease in Debye length results from increased electron number density with a rise in gas pressure. Consequently, the cathode sheaths become more confined. This directly impacts the plasma's ability to screen electric fields. As the Debye length decreases, the plasma becomes more efficient at neutralizing electric potentials within shorter distances, leading to enhanced electrostatic interactions between charged particles [24].

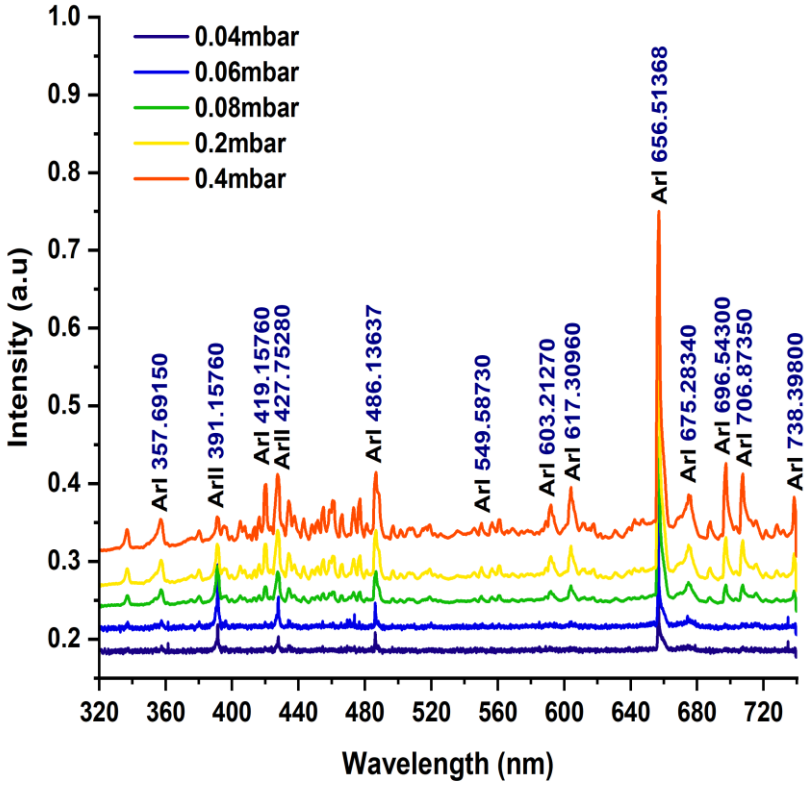


**Figure 6:** The variation of $\lambda_D$ with working pressure in planar magnetron sputtering.

### 4.3 Plasma Diffusion

#### 4.3.1 E×B Drift Velocity (Drift Wave Instability)

The drift velocity of charged particles in plasma is affected by gas pressure, which influences the mean free path of these particles. The drift velocity can be determined using Equation (4). Figure (7) illustrates the effect of gas pressure on drift velocity. The data showed that the drift velocity decreases as the gas pressure increases. This reduction can be attributed to the influence of the space charge formed near the electrode surface, which leads to a decrease in the value of $V_{E\times B}$. The space charge modifies the local electric field, reducing the drift velocity of charged particles and thus lowering the magnitude of $V_{E\times B}$, which represents the electric field associated with the ion drift in the presence of a magnetic field. Ions and electrons drift along the magnetic field due to $\nabla B \parallel B$. Charge separation caused by azimuthal electron drift in a planar magnetron can lead to plasma oscillations. This interaction with the magnetic field creates a radial drift, resulting in drift wave instability, where the perturbation electric field and magnetic field interact, destabilizing the plasma [25].

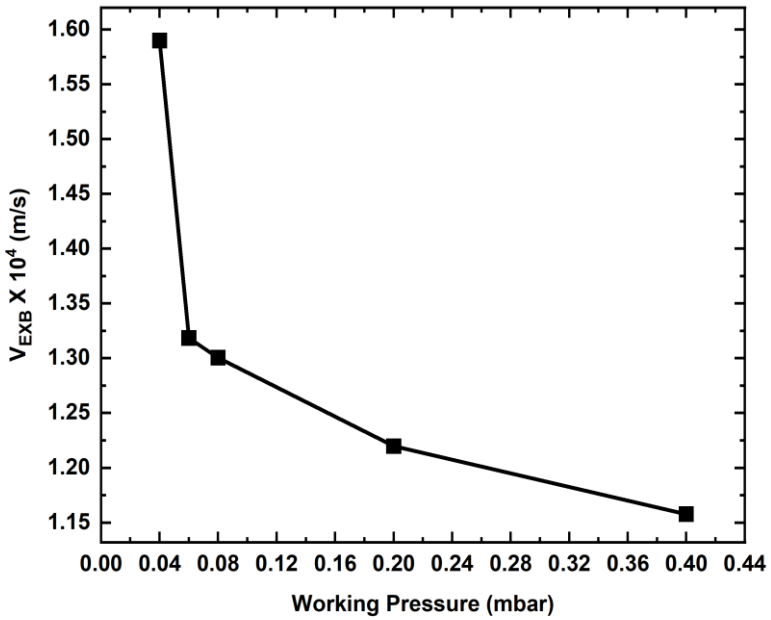


**Figure 7:** drift velocity versus working pressure.

### 4.3.2 Diffusion Coefficient and Constant Time Decay

The diffusion coefficients of drift wave turbulence can be influenced by several factors, including gas pressure. The diffusion coefficient measures how quickly particles or perturbations spread due to random motion or turbulence. Figure (8) presents the experimental values for the diffusion coefficient (calculated using Equation (5)) and the constant time decay (calculated using Equation (6)) as a function of working pressure. The data revealed that the diffusion coefficient decreased with rising gas pressure. As gas pressure increases, the density of the gas increases because the number of gas molecules per unit volume rises. This increase in density leads to more frequent collisions involving charged particles (electrons, ions, and neutrals), which can impede the motion of individual particles. Therefore, as pressure increases, the mean free path decreases, reducing the diffusion coefficient because particles have shorter distances to travel before colliding with others [26]. Additionally, the constant time decay increases with increasing gas pressure. This means that as the density of charged particles in the plasma increases with increases in gas pressure, collisions among particles become more frequent. This can lead to faster redistribution of momentum and energy, thereby decreasing the time decay constant. In general, increased density promotes quicker relaxation processes due to the higher likelihood of collisions [27].

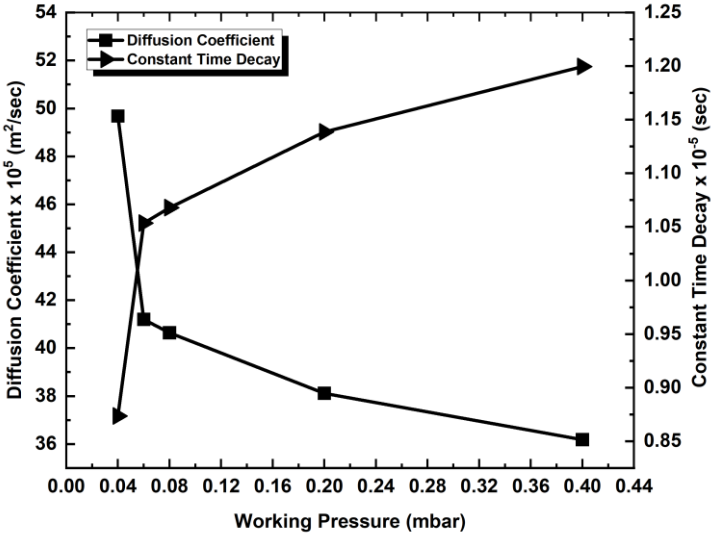


**Figure 8:** Diffusion coefficient and constant time decay of plasma as a function of working pressure.

### 4.3.3 Growth Rate and Particle Flux

The growth rate of drift wave instability as a function of working pressure depends on various factors, such as plasma parameters. The growth rate was calculated according to Equation (7). In addition, gas pressure can impact the particle flux related to drift wave instabilities by affecting the plasma density profile and the nature of the instability. Particle flux was calculated using Equation (8). Figure (9) shows how gas pressure influences growth rate and particle flux. The data showed a decrease in growth rate and particle flux with increasing gas pressure. This means that the growth rate decreases due to increased damping from more frequent collisions and reduced ability to sustain perturbations [28]. In addition, the particle flow decreases as a result of increased collision, which reduces efficient transport and spread in plasma. As the pressure on the gas increases, the increased density and frequency of conflict provide a more viscous environment for particles, slows the speed and reduces both growth and particle flow in the plasma [29].

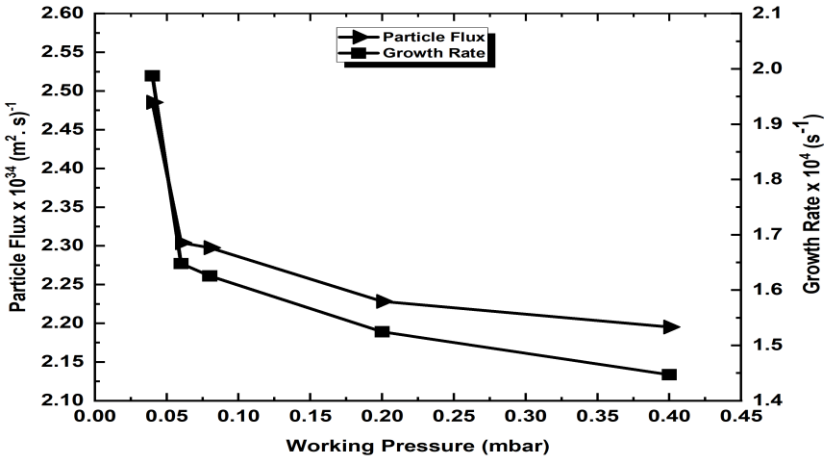


**Figure 9:** Growth rate and particle flux of drift wave instability as a function of working pressure.

## Conclusions

The main conclusion of the study is that the gas pressure has a significant effect on the properties of plasma in a DC glow discharge system. As gas pressure increases, the electron temperature ($T_e$) and Debye length ($\lambda_D$) decrease while the electron number density ($n_e$) increases. The emission strength of ArI and ArII lines also increases with higher gas pressure. Plasma diffusion is strongly influenced by gas pressure, with parameters such as drift velocity, diffusion coefficient, growth rate, and particle flux decreasing, while the time decay constant increases. The optimum conditions for plasma diffusion can be observed at the lowest gas pressure (0.04 Torr), where diffusion and other related parameters are more favorable. This work can be used in areas where precise control of plasma properties is required, such as material processing (e.g. etching, deposition), plasma therapy, and plasma-based diagnostics and is also useful in applications requiring plasma dynamics well, such as semiconductor manufacturing and surface treatment methods.

## References

**[1]** T. H. Khalaf , Q. A. Abbas, & M. M. Kadhim, "Study of Rod-Plate DC Discharge Plasma Characteristics at Atmospheric-Pressure," *Iraqi Journal of Science*, vol. 63, no. 11, pp. 4771-4778, 2022.

**[2]** M. M. Kadhim, Q. A. Abbas, , & M. R. Abdulameer, "Study of some plasma characteristics in dielectric barrier discharge (DBD) system," *Iraqi Journal of Science*, vol. 63, no. 5, pp. 2048-2056, 2022.

**[3]** M. M. Kadhim, & Q. A. Abbas, "The Influence of the Magnetic Field on the Plasma Characteristics in Hollow Electrodes Discharge System," *Iraqi Journal of Science*, vol. 63, no. 10, pp. 4254-4266, 2022.

**[4]** Q. A. Abbas, & R. T. Ahmead, "Diagnostics of dusty plasma properties in planar magnetron sputtering device," *Iraqi Journal of Physics*, vol. 13, no. 26, pp. 64-75, 2015.

**[5]** A. K. Bard, & Q. A. Abbas, "Influence of Cylindrical Electrode Configuration on Plasma Parameters in a Sputtering System," *Iraqi Journal of Science*, vol 63, no. 8, pp. 3412-3423, 2022.

**[6]** M. M. Kadhim, & Q. A. Abbas, "Plasma Instability Effect in Magnetron Sputtering Discharges Using Bohm Diffusion Analysis," *Iraqi Journal of Applied Physics*, vol. 20, no. 3, pp. 696-700, 2024.

**[7]** X. Liu, F. Wu, H. Chen, and X. Zhou, "Effects of electrode size and gas pressure on plasma uniformity in DC glow discharge systems," *Plasma Science and Technology*, vol. 23, no. 8, p. 084007, 2021.

**[8]** S. Chaudhary, P. Singh, and S. Thakur, "Optimization of plasma symmetry in DC glow discharge for improved mechanical performance," *Journal of Applied Physics*, vol. 128, no. 3, pp. 1-7, 2020.

**[9]** D. M. Devia, L. V. Rodriguez-Restrepo, and E. Restrepo-Parra, "Methods Employed in Optical Emission Spectroscopy Analysis," Ing. y Cienc., vol. 11, no. 21, pp. 239–267, 2015.

**[10]** S. S. Hamed, "Spectroscopic Determination of Excitation Premixed Laminar Flame," *Egypt J. Solids*, vol. 28, no. 2, pp. 349-357, 2005.

**[11]** H.R. Griem, "Principles of Plasma Spectroscopy," *Cambridge University Press*, pp. 1-345, 1997.

**[12]** L.A. Sobelman, "Excitation of Atoms and Broadening of Spectral Lines," *Springer-Verlag Berlin Heidelberg, New York*, pp. 1-200, 1979.

**[13]** H.R. Griem, "Spectral Line Broadening by Plasma," *Academic Press, New York*, pp. 1-300, 1974.

**[14]** N. M. Shaikh, S. Hafeez, B. Rashid, and M. A. Baig, "Spectroscopic studies of laser induced aluminum plasma using fundamental, second and third harmonics of a Nd: YAG laser," *Eur. Phys. J. D*, vol. 44, no. 2, pp. 371–379, 2007.

**[15]** K. H. Spatschek, "Introduction to Theoretical Plasma Physics," *Lecture Series*, pp. 1-30, 2008.
**[16]** R. J. Goldston and P. H. Rutherford, "Introduction to Plasma Physics," *CRC Press*, pp. 89–92, 1995.
**[17]** K. S. K. Srivastava, "Diffusion Processes in Plasma Physics," *Journal of Plasma Physics*, vol. 80, pp. 15–22, 2014.
**[18]** M. A. Lieberman and A. J. Lichtenberg, "Principles of Plasma Discharges and Materials Processing," *Wiley-Interscience, New York*, pp. 1-300, 2005.
**[19]** J. P. Freidberg, "Plasma Physics and Fusion Energy," *Cambridge University Press*, pp. 115–118, 2007.
**[20]** P. M. Bellan, "Fundamentals of Plasma Physics," *Cambridge University Press*, pp. 1-400, 2006.
**[21]** Q. A. Abbas, A. F. Ahmed, F. A.-H. Mutlak, "Spectroscopic analysis of magnetized hollow cathode discharge plasma characteristics," *Optik - International Journal for Light and Electron Optics*, vol. 242, pp. 167260, 2021.
**[22]** NIST Atomic Spectra Database. [Online]. Available: https://www.nist.gov/pml/atomic-spectra-database, Accessed: 2024.
**[23]** M. A. Hassouba, "Effect of the magnetic field on the plasma parameters in the cathode fall region of the DC-glow discharge," *The European Physical Journal Applied Physics*, vol. 14, no. 2, pp. 131-135, 2001.
**[24]** B. B. Sahu, K. Bera, and L. N. Mishra, "Effect of gas pressure on Debye length and sheath dynamics in low-pressure glow discharge plasmas," *Physics of Plasmas*, vol. 27, no. 12, pp. 123502, 2020.
**[25]** S. Kumar, S. K. Mishra, and R. Tiwari, "Influence of gas pressure on drift velocity and plasma oscillations in planar magnetron discharges," *Physics of Plasmas*, vol. 28, no. 7, pp. 073505, 2021.
**[26]** K. Trachenko, and V. V. Brazhkin, "Molecular dynamics of gases at high pressures: Mean free path and diffusion," *Science Advances*, vol. 6, no. 45, eaba3747, 2020.
**[27]** P. J. Bruggeman, M. J. Kushner, B. R. Locke, J. G. E. Gardeniers, W. G. Graham, D. B. Graves, R. C. H. M. Hofman-Caris, D. Maric, J. P. Reid, E. Ceriani, and M. G. Kong, "Plasma–liquid interactions: A review and roadmap," *Plasma Sources Science and Technology*, vol. 29, no. 10, pp. 103001, 2020.
**[28]** H. E. Nieminen, E. K. J. Kilpua, and D. Laviron, , "Gas pressure effects on particle flux and growth rates in dusty plasmas," *Journal of Physics D: Applied Physics*, vol. 53, no. 47, pp. 475202, 2020.
**[29]** N. Bazou, J. Fernández, J. Cotrino, and M. Shiratani, "Influence of gas pressure on particle transport and growth in capacitively coupled plasmas," *Plasma Processes and Polymers*, vol. 18, no. 4, e2100003, 2021.